New Gold and Silver-Gold Catalysts in the Shape of Sponges and Sieves

Birte Jürgens[1], Christian Kübel[2], Christian Schulz[1], Tobias Nowitzki[1], Volkmar Zielasek[1], Jürgen Biener[3], Monika M Biener[3], Alex V Hamza[3], Marcus Bäumer[1]

[1] University of Bremen, Institute of Applied and Physical Chemistry, Leobener Str. NW2, 28359 Bremen, Germany

[2] Fraunhofer Institute for Manufacturing Technology and Applied Materials Science (IFAM), Adhesive Bonding and Surfaces Division, Wiener Straße 12, 28359 Bremen, Germany

[3] Lawrence Livermore National Laboratory, Livermore, CA 94550, United States of America

Email: mbaeumer@uni-bremen.de

Abstract

Gold with a nanoporous sponge-like morphology, generated by leaching of AuAg alloys is presented as a new unsupported material system for catalytic applications. The role of residual silver for catalytic activity towards CO oxidation in the temperature range from -20 to 50°C has been investigated by comparison with Au and Au/Ag zeolite catalysts. As revealed by a systematic variation of the silver content in the zeolite catalysts, bimetallic systems exhibit a significantly higher activity than pure gold, probably due to activation/dissociation of molecular oxygen by silver. By STEM tomography we can unambiguously prove that at least some of the particles form inside the zeolite lattice.

Keywords

Introduction

Gold exhibits interesting catalytic properties as demonstrated, e.g., for the selective oxidation of olefins or CO oxidation at low temperatures (1-11). So far, research in this field has focused mainly on gold in the shape of nanoparticles on suitable oxide supports. Many different support materials have been tested in this way, TiO_2 perhaps being the most intensively studied so far (8-11). The mechanisms leading to catalytic activity are still being debated, due to the complexity of particle-support interaction and reaction pathways. So far, it has been shown that particle size, support material, and particle-support contact structure play major roles (6,11,12).

We now describe two other approaches which have received much less attention so far. The first material which we will discuss in this paper is a nanoporous gold foam as an example of an *unsupported* gold system. The other system is a gold-loaded zeolite where Au particles larger than the cages of the zeolite structure could be prepared *inside* the zeolite. In both cases, Ag as an additional component plays a role and its influence will be discussed.

In the past, unsupported gold has been studied as a catalytic material only in a few cases (13,14) although it holds out interesting prospects for technical applications and furthermore may lead to more detailed insights into basic catalytic mechanisms. Recently, we demonstrated that *unsupported* nanoporous gold, generated by leaching of AgAu alloys, exhibits significant catalytic activity with respect to CO oxidation at temperatures as low as 0°C (15). Since Ag cannot be completely removed from the material, it has been speculated in this study that Ag residues at the surface of the nanoporous foam are involved in the catalytic cycle. In the following, we will describe this work and compare the results to the zeolite-based system where the influence of the Ag could be investigated in a systematic manner.

Gold-loaded zeolites were prepared even 20 years ago (16). In spite of their promising catalytic properties, it turned out, however, that it is difficult to obtain stable systems with respect to sintering. This problem was solved by Guillemot and co-workers in 1996, who were able to prepare small and thermally stable gold particles located in the $Na_xH_{x-1}Y$ zeolite lattice using reduction of Au^{III} by its ligands (17). Following such an approach, we prepared Au and Au/Ag particles inside the zeolite lattice. Since the bimetallic particles were prepared by subsequently doping the Au loaded system with Ag, such systems have permitted us to deliberately vary the Ag-Au particle composition. While it will be shown that monometallic gold shows already good activity towards CO oxidation even at room temperature, a variation of the particle composition in the zeolites reveals that the CO to CO_2 turnover may be enhanced by up to 100% if the Ag content is properly chosen. Probable mechanisms will be discussed.
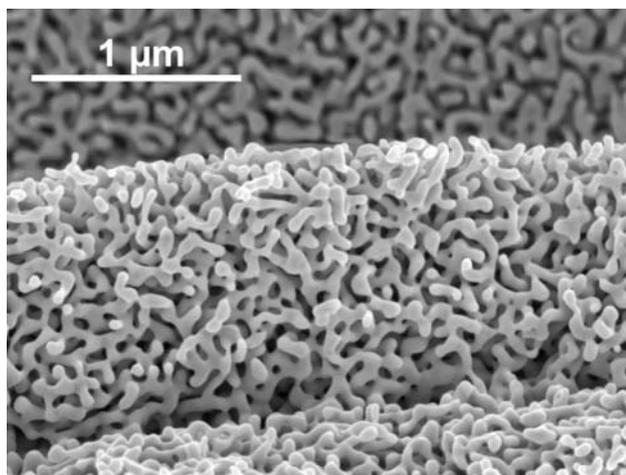
Figure 1

Scanning electron micrograph of nanoporous gold showing a sponge-like morphology with ligaments that are some 10 nm wide

Experimental

Sample preparation and characterization

Nanoporous gold with a specific surface area of ~ 4 m^2/g was obtained by selective dealloying of an AuAg alloy (70% Ag) in 70% concentrated nitric acid (18). By complex processes involving leaching of Ag and large-scale rearrangements of the resulting vacancies and Au adatoms (19), a sponge-like morphology was obtained which exhibits interconnecting ligaments with diameters in the order of several tens of nanometers (Figure 1). The ligaments consist of smaller grains as revealed by transmission electron microscopy (TEM) (see (18) for further details). The nanoporous gold samples used in our experiments have a residual Ag bulk content of ~ 1% as determined by atom absorption spectroscopy (AAS) after dissolution in HCl/HNO$_3$.

Nanoparticles of gold in Y-zeolites were prepared according to Chen *et al*. (20). The Y-zeolites (Union Carbide) were first calcined at 550°C for 4 hours. Then their surface acidity was adjusted by a long-term (2 days) immersion in a nitric acid bath (pH=6) at room temperature before the zeolites were washed nitrate-free and finally dried at 60°C. The zeolites were loaded with gold by submerging them in chloroauric acid solution at 80°C for 16 hours after the pH of the solution had been carefully adjusted to 6 by adding NaOH. The gold-loaded zeolites were filtered, washed to remove chloride, and finally dried at 60°C. However, subsequent calcination at higher temperatures was not used. The gold content of the catalysts was confirmed by AAS. Below we designate the Au-loaded zeolite samples as AuY.

Bimetallic silver-gold nanoparticles were obtained by submerging AuY in AgNO$_3$ / water for 30 minutes (21), leading to quantitative uptake of silver as revealed by AAS. During this preparation step the pH was carefully controlled. The zeolites were washed to remove nitrate and subsequently dried at 60°C. Below we designate Ag/Au-loaded zeolite samples as Ag/AuY. The silver content was varied by the concentration of the AgNO$_3$ solution used. Samples with Ag:Au weight proportions of 1 : 1, 0.6 : 1, 0.3 : 1 and 0.1 : 1 were investigated in this study. The specific surface area of all AuY and Ag/AuY samples was determined as about 700 m^2/g by a conventional volumetric BET method (nitrogen adsorption). An overview of relevant parameters for all samples used in this study is given in Table 1.

As discussed in the 'Results and discussion' section, the Au/Ag loaded zeolites were carefully characterized by TEM, using a Technai F20 ST with a nominal resolution of 0.2nm in STEM mode. High Angle Annular Dark Field Scanning Transmission Electron Microscopy (HAADF-STEM) in combination with Energy Dispersive X-ray (EDX) microanalysis of individual particles was performed to check their composition. These spectra clearly revealed that Ag intermixes with Au to form bimetallic particles. No monometallic silver particles were found.

Catalytic measurements

For the catalyst activity evaluation experiments, a continuous flow reactor made from glass tubing was used and heated in a silicone oil bath or cooled in a NaCl/water ice bath as required. Nanoporous gold samples (80 mg, thickness 300 μm, diameter about 10 mm) were placed on a ceramic frit inside the glass tubing. The zeolite samples were slightly

Table 1

Overview of sample parameters for nanoporous gold (Au sponge) and zeolite catalysts (AuY and Ag/AuY). The weight fractions have been determined by AAS

	Au-sponge	AuY	Ag/AuY 0.1 : 1 (19 at% Ag)	Ag/AuY 0.3 : 1 (36 at% Ag)	Ag/AuY 0.6 : 1 (53 at% Ag)	Ag/AuY 1 : 1 (66 at% Ag)
BET surface [m^2/g]	3.7	697.5	614.7	734.3	682.8	659.7
Ag : Au (weight)	0.7% : 99.3%	0% : 100%	11.6% : 88.4%	23.2% : 76.8%	38.6% : 61.4%	51.5% : 48.5%
Ag : Au (molar)	1.3% : 98.7%	0% : 100%	19.3% : 80.7%	35.6% : 64.4%	53.4% : 46.6%	66.0% : 34.0%
	XPS: 4% - 20%					
total metal content in sample (mg)	80	3	3	3	3	3

pressed and chunks of 0.32 to 0.45 mm diameter (total metal content ~3 mg) were placed into the tubing and held in place by glass wool. The reactant flow was varied between 0.5 and 8.5 vol% CO in dry synthetic air (80% N_2/20 %O_2, H_2O concentration < 5 ppm). The total gas flow was 15 mL/min for the nanoporous gold samples and 50 mL/min for the zeolite samples, respectively. (Note that, with the nanoporous gold samples, it could not be avoided that part of the reactant gas by-passed the sample.) An infrared-gas-analyser (IRGA) was used to quantify the amount of CO_2 present after the gas flow had passed the catalyst.

Results and discussion

Unsupported nanoporous gold

In the CO oxidation experiments with the freshly prepared
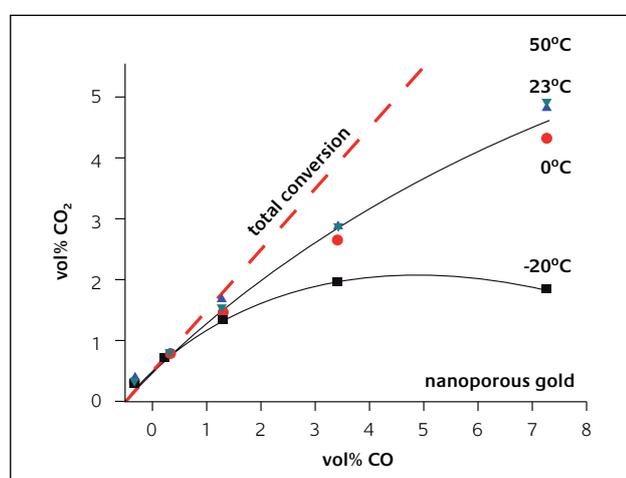
Figure 2
Dependence of the CO_2 concentration at the outlet on the admitted CO concentration at the inlet (dashed line marks total conversion) for nanoporous gold. At temperatures of 0°C and higher the conversion reaches about 3/5 at CO concentration of 8%. Only at -20°C the conversion apparently saturates at about 2%CO_2
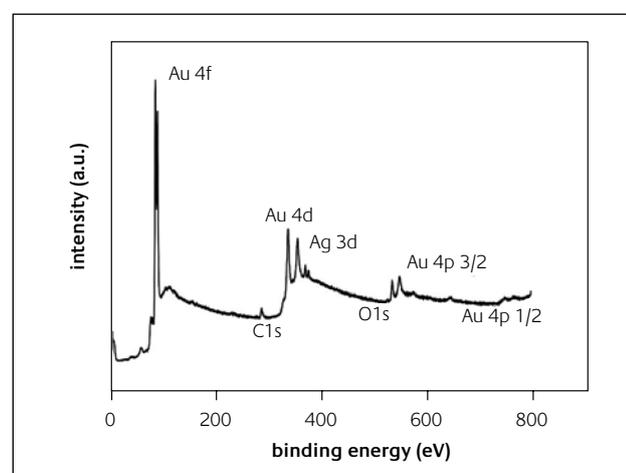
Figure 3
XP spectrum of a nanoporous gold sponge after catalytic experiments proving the presence of silver at the surface

nanoporous gold samples, an increase of the IRGA CO_2 signal was observed after an activation period of ~30 minutes at 50 - 75°C, indicating the onset of catalytic activity which then gradually increased over several hours. It is probable that, during the activation period, contaminants derived from the leaching process are removed. Once activated at elevated temperatures, the nanoporous gold samples show immediate catalytic activity even at low temperatures (15). Figure 2 shows the dependence of the CO_2 concentration in the reactor outlet on the CO concentration admitted in the inlet for temperatures in the range -20 to 50°C. This range is particularly interesting with respect to applications of gold for low-temperature catalysis. For up to 2% CO, the CO_2 yield indicates total conversion. At temperatures of 0°C and above, a continuous increase of the CO_2 concentration with the levels of CO admitted is observed, and at 8% CO still 5/8 is converted to CO_2, showing an unexpectedly high activity for an unsupported gold catalyst. More recently, catalytic activity of nanoporous gold has also been reported by others (22). Xu *et al.* admitted 1% CO in a fixed-bed reactor and used gold foams prepared by electrochemical dealloying which generates ligaments of somewhat smaller sizes as compared to our samples.

As indicated by studies on supported AuAg alloy particles (23) and on Ag-contaminated Au powders (13), the residual silver atoms left after the dealloying process may have a significant effect on the catalytic activity. In fact, x-ray photoelectron spectroscopy (XPS) reveals in our studies that the residual silver content is enhanced close to the surface of the ligaments to between 4 and 20%, depending on the sample (see Figure 3). Additionally, only minor surface contaminations by carbon and oxygen were detected, probably due to hydrocarbon- and OH-species (the spectrum shown in Figure 3 was taken after several days of CO oxidation).

Unfortunately, the controlled preparation of unsupported gold sponges with varying Ag/Au ratios is by no means trivial and is the subject of current research (24). In the case of the zeolite-based system, however, the Au/Ag ratio can be systematically varied. The CO oxidation results indeed show a significant influence of the silver on the catalytic activity, as will be demonstrated below.

AuY and Ag/AuY zeolites – comparison with nanoporous gold

The freshly prepared Au- and Au/Ag-loaded zeolites were carefully characterized by TEM. The images in Figure 4a) (AuY) and b) (Ag/AuY) reveal that in both cases particles with a diameter of about 2-5 nm form. For the bimetallic system, HAADF-STEM imaging in combination with x-ray microanalysis of individual Au/Ag nanoparticles presented in Figure 4c shows nanoparticles with a slightly varying silver content, but in no case did we observe pure silver nanoparticles. Single 2D projection images do not allow to differentiate between metal particles located on the *outer* surface of the matrix and those incorporated *inside* the zeolite cages. We solved this
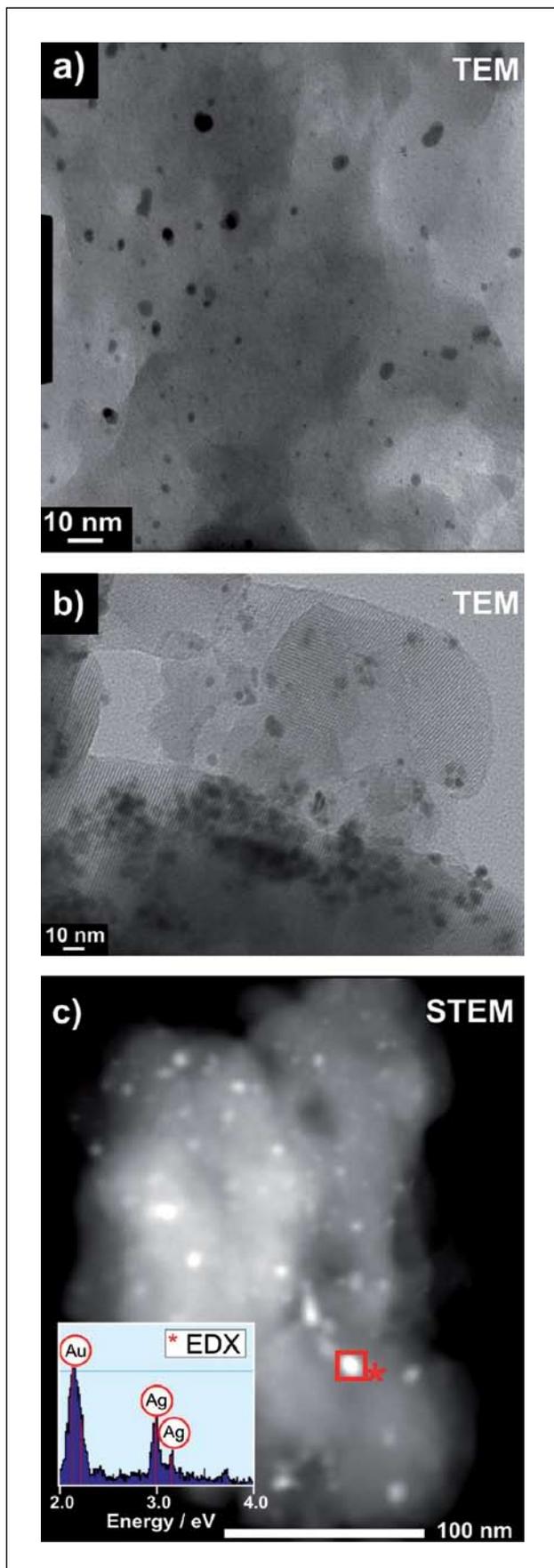
Figure 4

TEM of freshly prepared a) Y-zeolites with Au nanoparticles and b) Y-zeolite with bimetallic Ag/Au nanoparticles (weight ratio: 0.6 : 1). Image c) shows a STEM image of a Au/Ag loaded zeolite (weight ratio 1 : 1) with an EDX spectrum (inset) of the marked particle
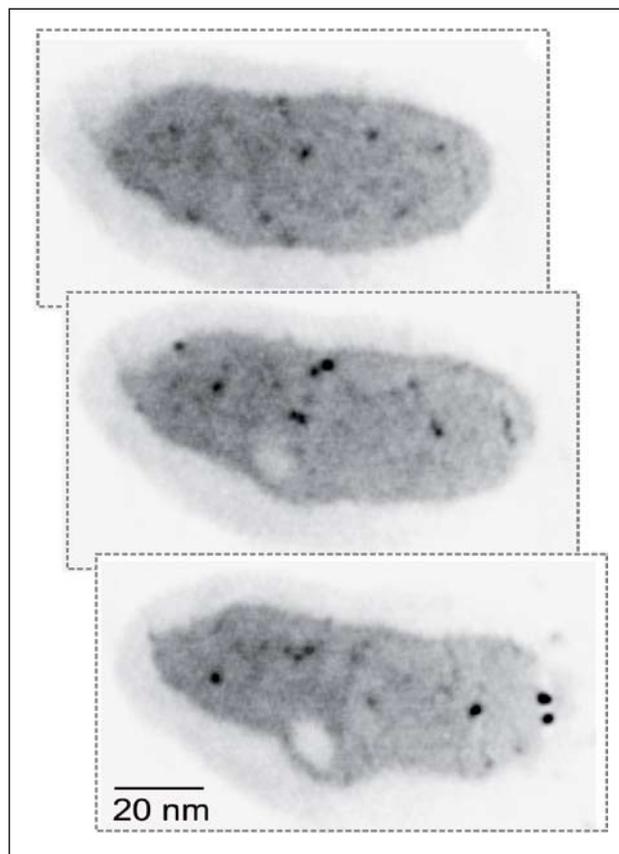
Figure 5

Three slices of the electron tomographic reconstruction of a crystallite loaded with Ag/Au nanoparticles. The slices intersect the crystallite close to its centre and clearly show that metal nanoparticles (black dots) are located inside the crystallite

problem by using electron tomography (25-28) to obtain a full 3D representation of the matrix loaded with catalyst particles. Only recently, this technique has emerged as a powerful tool to study catalytic materials as, for instance, demonstrated for AgY (26) or, in combination with x-ray microanalysis, for bimetallic particles in mesoporous silica (27,28). First, a set of 86 HAADF-STEM images taken of a single zeolite crystallite over a tilt-range of ±70° was acquired. After aligning the images, the 3D structure of the crystallite with the catalyst particles was reconstructed digitally, using the SIRT algorithm. Figure 5 shows three slices *through* this crystallite, clearly establishing that some particles (black spots) are *incorporated* in the zeolite lattice. Since their sizes have been determined to be between 2 and 3 nm, they exceed the pore sizes of the Y-zeolite. Other particles being larger were located on the outer surface.

At first sight it may be surprising that we find the formation of particles in our experiments although no reduction step with, for example, hydrogen was employed. Instead, ionic species bound to the zeolite lattice by ion exchange might be expected. (Note that also in the case of gold, an exchange reaction is possible since, according to Kang and co-workers, zero-charged $AuCl_{3-x}OH_x$ gold complexes formed at elevated pH can be involved in such a process (29).) In several instances, reduction of these ionic species resulting in

metal particles has been observed even at low temperatures and explained by 'autoreduction', i.e., the residual water or the ligands of the precursor may act as a reducing agent under these conditions (16,17,30-32). In the case of silver, this process is photocatalytically induced as reported in the literature (31).

A second point which requires discussion is the formation of particles within the zeolite lattice which are larger than the dimensions of the cage sizes. In this context, it is important to note that Jaeger *et al.* (33,34) obtained similar results for other metallic particles (Ni, Pt, Pd, Ru). In these cases a calcination step (in air at about 400°C) was used to remove the ligands (33,34). During this process, the metal cations migrate into the sodalite cages. In a subsequent reduction step (under hydrogen at about 350°C) metallic particles are finally formed. The mechanism proposed by these authors in order to explain the enlargement of the cages is based on a local destruction of the zeolite lattice by protons resulting

from the reduction step (33,34). For an AuY system prepared from a different Au precursor by autoreduction, a similar explanation has been provided by Guillemot *et al* (17,35). Thus, it can be assumed that such a scenario is responsible for the formation of particles exceeding the regular cage sizes in our case as well.

Although the TEM data unambiguously prove the existence of metal particles in the zeolites, it is an open question as to whether residual ionic species are still present in the lattice as well. Our catalytic experiments suggest that this may be the case. In contrast to nanoporous gold, freshly prepared metal-loaded zeolites (both mono- and bimetallic systems) do not require activation, but show immediate catalytic activity for CO oxidation. In the case of the gold-loaded zeolite, however, the observed activity continuously increased over the first 4 hours until a constant steady-state activity was reached. A similar behaviour was reported by Chen *et al.* for CO oxidation on AuY and interpreted in terms of an ongoing reduction of residual ionic Au species in the lattice to metallic gold by CO (20). Based on these findings, these authors came to the conclusion that *metallic* gold is the catalytically active species. It is interesting to note that this interpretation is in clear contrast to that of Kang *et al.* who, on the basis of their work, claim *ionic* gold to be the active species (29). Based on the similarities with respect to the initial activity increase, our results support the view of Chen *et al.* So, ionic species which are probably present at the beginning of our catalytic experiments seem to be inactive under the reaction conditions used. Instead, the formation of metallic gold particles appears to be necessary. Interestingly, we did not detect such an induction period for CO oxidation with the bimetallic system, suggesting that here less ionic species were present after preparation.

Figure 6 a) shows the steady state activities for CO oxidation as a function of the CO concentration for an AuY catalyst and an Ag/AuY catalyst (Ag/Au weight ratio: 0.1:1, corresponding to 19 at% Ag) at room temperature. Compared to the turnover obtained for nanoporous gold (blue dashed line), the activities of the zeolites show the same trend, i.e., the CO_2 concentration continuously increases as the concentration of CO admitted increases. In comparison, Haruta *et al.* found almost no dependence of the turnover frequency on CO concentration (range: 0.1 – 10 vol%) in their studies of supported Au particles, and concluded that the CO oxidation follows a Langmuir-Hinshelwood mechanism with the surface reaction being the rate-limiting step (11). Consequently, oxygen and CO would saturate the catalyst surfaces and the kinetic order of the reaction should be zero. In our experiments for both, nanoporous gold and zeolites, however, the CO_2 yield clearly increases with CO concentration, indicating that the CO oxidation at the surface is likely limited by *gas transport* and not by surface reaction. Therefore, in the case of nanoporous gold, the pore sizes should not be too small for a high overall catalytic performance. If a material with pore sizes in the range of a few nanometers is chosen, as described by Xu *et al.* (22), the benefit of an increased surface area is

(a)

(b)
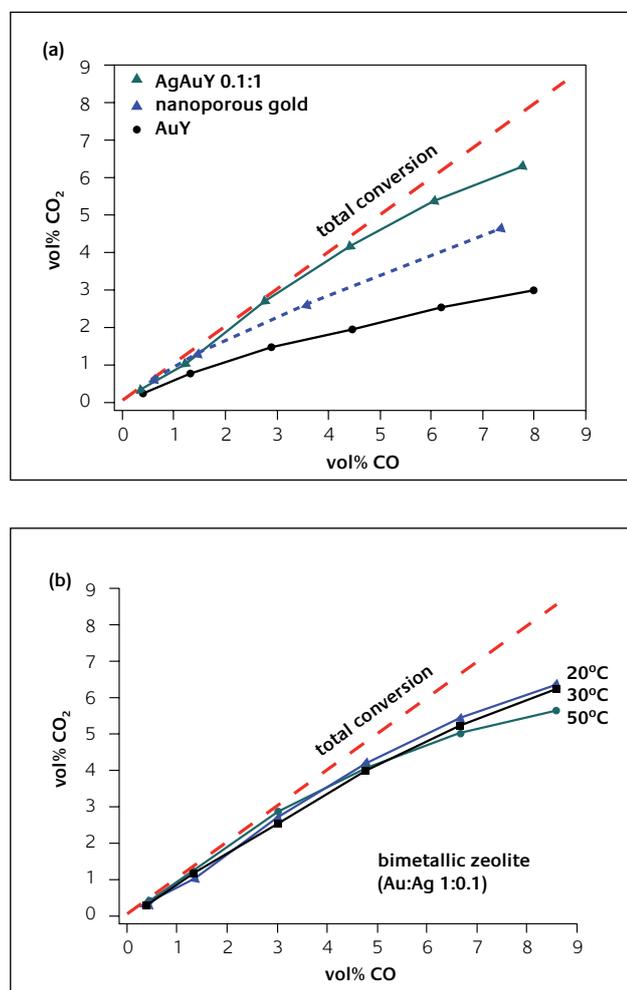
Figure 6

Dependence of the CO_2 concentration at the outlet on the admitted CO concentration (0.5% to 8.5%) at the inlet. a) AuY and Ag/AuY (Ag/Au weight ratio: 0.1:1, 19 at% Ag) catalysts at room temperature. The results for nanoporous gold are shown for comparison (see text for details). b) Bimetallic (AgAuY) zeolite at different temperatures (20°C, 30°C and 50°C). Up to 3% CO nearly total conversion is observed, and at 8.5% CO the conversion rate is about 75% for all temperatures
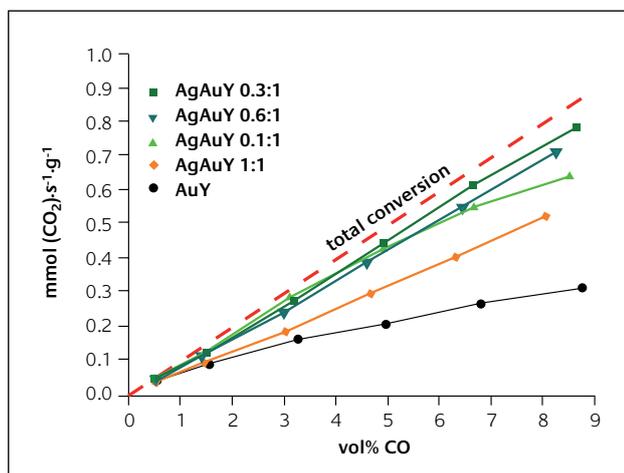
Figure 7

CO to CO$_2$ conversion (mmol CO$_2$ formed per g metal and second plotted as a function of vol% CO admitted) at room temperature as a function of the Ag/Au weight ratio (range 0.1:1 to 1:1 corresponding to 19 at%, 36 at%, 53 at% and 66 at% of Ag) for the zeolite catalysts. The activity of bimetallic catalysts is higher than that of monometallic AuY catalysts for all Ag amounts studied. The AgAu ratio 0.3:1 (36 at% Ag) shows the best performance

probably counterbalanced by hindered gas transport to the active surface sites.

Similar to nanoporous gold, the zeolite catalysts do not exhibit any significant dependence on temperature in the range 20 to 50°C, as shown in Figure 6 b) for Ag/AuY with an Ag/Au weight ratio of 0.1:1 (19 at% Ag). The saturation of the CO$_2$ yield for nanoporous gold at -20°C visible in Figure 2 indicates that at such low temperatures an elementary step of the CO oxidation, probably the dissociation of O$_2$, is limiting the conversion.

It should be noted here that the CO$_2$ yields from the zeolite catalysts and those of nanoporous gold at room temperature are shown together in Figure 6 a) to demonstrate the same trend. A quantitative comparison is impossible, since for nanoporous gold part of the reactants could bypass the catalyst. For both zeolite catalysts, however, the CO$_2$ yield can be directly compared, revealing that the activity of the AuY catalyst (monometallic gold particles) is about 50% of that of Ag/Au-Y (Ag/Au weight ratio 0.1:1, 19 at% Ag). In this context, it is important to note that silver alone is not active towards CO oxidation under the conditions used (36-38). In order to confirm this for our specific system, we performed experiments with a zeolite sample, containing 2%wt of silver. Briefly, we detected no activity for CO oxidation at temperatures below 100°C. So, while pure gold loaded zeolites already show high catalytic activity, silver can significantly enhance the performance of the AuY catalysts.

Figure 7 shows the CO to CO$_2$ conversion for bimetallic Ag/AuY-zeolites of different Ag/Au ratios at CO admission levels between 0.5% and 8.5%. All measurements were carried out at room temperature. (For comparison with other studies, the amount of CO$_2$ is given in mmol formed per second and gramme metal.) The data reveal that the 0.3:1 Ag/Au weight ratio (36 at% Ag) gives the best turnover, very close to total

conversion even for 8.5% CO. The activity is lower when the Ag/Au weight ratio is increased to 0.6:1 (53 at% Ag), or when it is decreased to 0.1:1 (19 at% Ag).

A reasonable explanation for how silver promotes the catalytic activity of the gold catalyst is the supply of surface sites for O$_2$ dissociation (39-41) while CO adsorbs at low-coordinated gold sites (42). Wang *et al.* speculated in this context that molecular oxygen is activated by electron transfer to the antibonding π orbitals at silver sites, leading to the formation of O$_2^-$ species (23). In their experimental studies of the activity of MCM-supported bimetallic Ag/Au particles towards CO oxidation at room temperature, they also find a strong dependence of the catalytic activity on the Ag/Au ratio. In their experiments, however, the particles were relatively large as compared to our case, and they allowed only for 1% CO admission levels. While our findings are in good accordance, we have expanded the range of CO admission concentrations of up to 8.5% CO and show that the results are applicable even at low temperatures for small bimetallic particles as those incorporated in the cages of Y-zeolites.

Conclusion

Our experiments reveal high catalytic activity of nanoporous gold and bimetallic Ag/Au Y-zeolites in the temperature range 0 to 50°C with respect to CO oxidation. The dependence of the activity on CO admission concentrations and on temperature shows the same trend in both cases, indicating that the catalytic mechanisms are quite comparable. The activity of the zeolite catalysts is significantly enhanced by the presence of *silver*. A silver content of about 4 – 20% at the surface is probably also responsible for the high catalytic activity of the nanoporous gold which can be used as an *unsupported* gold catalyst. It is not yet clear whether Ag intermixes with Au or forms islands on the surface. The distribution of the silver atoms could play an important role in the catalytic mechanism. Subsurface oxygen may form in the case of larger Ag patches and is known to influence the reactivity of surface oxygen (43).

By performing a 3D STEM tomography analysis it was possible to prove that gold and bimetallic gold silver nanoparticles even larger than the cages of the unloaded zeolite can be incorporated in the zeolite lattice which indicates an enlargement of the cages induced by the metal loading processes. The experiments with bimetallic Ag/Au Y zeolites have revealed that there exists an optimum Ag/Au weight ratio around 0.3 : 1 corresponding to 36 atom% of silver. Current investigations are taking place on the preparation of nanoporous gold samples with different Ag contents in order to validate these findings for the unsupported Au sponge.

Both, nanoporous gold and bimetallic Ag/Au zeolites are promising candidates for catalytic applications. The nanoporous gold is a catalyst in its own right, and thermally

and mechanically stable (44,45). The bimetallic zeolite systems are easily accessible and cost efficient because only very small amounts of gold are necessary due to the high surface to volume ratio. Furthermore, sintering of the particles, which is still a general problem for catalysis by Au-nanoparticles, may be prevented due to incorporation of the nanoparticles into the zeolite cavities.

About the authors

Marcus Bäumer is professor at the *Institute of Applied and Physical Chemistry* of the University of Bremen. He and Volkmar Zielasek, as a senior scientist, head a research group working in the border area between surface science and catalysis with a focus on chemical reactions at nanostructured surfaces, model catalytic studies, and innovative catalytic materials. Birte Jürgens, who was responsible for the preparation of the zeolite catalysts and the catalytic experiments described here, and Tobias Nowitzki are PhD students in this group. Christian Schulz is a former diploma student who worked with the gold foams.

Volkmar Zielasek

Christian Kübel is head of the electron microscopy group at *Fraunhofer IFAM* and is focusing on structural characterization and properties of (nano)materials. He has previously worked at Philips Natuurkundig Laboratorium / FEI and as a Feodor Lynen (AvH) fellow at the University of Michigan.

Alex Hamza and **Juergen Biener** are leaders in the Nanoscale Synthesis and Characterization Laboratory (NSCL) at the *Lawrence Livermore National Laboratory*. The NSCL develops and characterizes novel nanostructured materials such as nanoporous metals and nanocrystalline materials for high-power laser experiments.

References

1   M. Haruta, N. Yamada, T. Kobayashi and S. Iijima, *J. Catal.*, 1989, **115**, 301

2   T. Hayashi, K. Tanaka and M. Haruta, *J. Catal.*, 1998, **178**, 566

3   K. A. Davis and D. W. Goodman, *J. Phys. Chem. B*, 2000, **104**, 8557

4   A. K. Sinha, S. Seelan, S. Tsubota and M. Haruta, *Angew. Chem.*, 2004, **116**, 1572; *Angew. Chem. Int. Ed.*, 2004, **43**, 1546

5   T. A. R. Nijhuis, T. Visser and B.M. Weckhuysen, *Angew. Chem.* 2005, **117**, 1139; *Angew. Chem. Int. Ed.*, 2005, **44**, 1115

6   M. Haruta, *Catal. Today*, 1997, **36**, 153

7   G. C. Bond and D.T. Thompson, *Cat. Rev. - Sci. Eng.,* 1999, **41**, 319

8   R. Meyer, C. Lemire, Sh. K. Shaikhutdinov and H.-J. Freund, *Gold Bull.*, 2004, **37**, 72

9   M. Haruta and M. Daté, *Appl.* Catal. *A*, 2001, **222**, 427

10   M. Haruta, *Chem. Rec.*, 2003, **3**, 75

11   M. Haruta, *Cattech*, 2002, **6**, 102

12   T. V. Choudhary and D.W. Goodman, *Appl. Catal. A*, 2005, **291**, 32

13   Y. Iizuka, A. Kawamoto, K. Akita, M. Daté, S. Tsubota, M. Okumura and M. Haruta, *Catal. Lett.* 2004, **97**, 203

14   M. B. Cortie, E. van der Lingen and G. Pattrick, Proc. Asia Pacific Nanotechnology Forum 2003, Cairns Australia (World Scientific Press), Singapore, pp 79 – 82; L. Glaner, E. van der Lingen and M.B. Cortie, Australian Patent 2003/215039

15   V. Zielasek, B. Jürgens, Ch. Schulz, J. Biener, M.M. Biener, A.V. Hamza and M. Bäumer, *Angew. Chem. Int. Ed.*, 2006, **45**, 8241

16   D. Guillemot, V. Yu. Borovkov, V. B. Kazansky, M. Polisset-Thfoin and J. Fraissard, *J. Chem. Soc., Faraday Trans.* 1997, **93**, 3587 and citations therein

17   D. Guillemot, M. Polisset-Thfoin and J. Fraissard, *Catal. Lett.*, 1996, **41**, 143

18   A. M. Hodge, J. Biener, L. M. Hsiung, Y.M. Wang, A. V. Hamza and J. H. Satcher, J. *Mater. Res.*, 2005, **20**, 554

19   J. Erlebacher, M. J. Aziz, A. Karma, N. Dimitrov and K. Siederadzki, *Nature,* 2001, **410**, 450

20   J.-H. Chen, J.-N. Lin, Y.-M. Kang, W.-Y. Yu, C.-N. Kuo and B.-Z. Wan, *Appl. Cat. A*: *Gen.l,* 2005, **291**, 162

21   A similar procedure was previously used for loading A-zeolites with silver: R. Seifert, R. Rytz, and G. Calzaferri, *J. Phys. Chem. A,* 2000, **104**, 7473

22   C. Xu, X. Xu, P. Liu, H. Zhao, F. Tian, Y. Ding, *J. Am. Chem. Soc.*, 2007, **129**, 42

23   A.-Q. Wang, J.-H. Liu, S. D. Lin, T.-S. Lin and C.-Y. Mou, *J. Catal.*, 2005, **233**, 186

24   A. Wittstock, J. Biener, M. M. Biener, V. Zielasek, A. Hamza and M. Bäumer, in preparation

25 Ch. Kübel, A. Voigt, R. Schoenmakers, M. Otten, D. Su, T.-C. Lee, A. Carlsson and J. Bradley, *Microsc. Microanal.*, 2005, **11**, 378

26 A. J. Koster, U. Ziese, A. J. Verkleij, A. H. Janssen and K. P. de Jong, *J. Phys. Chem. B,* 2000, **104**, 9368

27 M. Weyland, P. A. Midgley, J. M. Thomas, *J. Phys. Chem.* B, 2001, **105**, 7882

28 P. A. Midgley, J. M. Thomas, L. Laffont, M. Weyland, R. Raja, B. F. G. Johnson and T. Khimyak, *J. Phys. Chem. B,* 2004, **108**, 4590

29 Y.-M. Kang and B.-Z. Wan, *Cat. Today,* 1997, **35**, 379

30 J. Texter, T. Gonsiorowski and R. Kellerman, *Phys. Rev. B,* 1981, **23**, 4407

31 P. A. Jacobs, J. B. Uytterhoeven and H. K. Beyer, *J. Chem. Soc., Chem. Comm.*, 1977, 128

32 S. Leutwyler and E. Schumacher, *Chimia,* 1977, **31**, 475

33 N. Jaeger, P. Ryder, G. Schulz-Ekloff, *Stud. Surf. Sci. Catal.*, 1984, **18**, 299

34 D. Exmer, N. Jaeger, R. Nowak, H. Schrubbers and G. Schulz-Ekloff, *J. Catal.*, 1982, **74**, 188

35 G. Riahi, D. Guillemot, M. Polisset-Thfoin, A. A. Khodadadi and J. Fraissard, *Catal. Today,* 2002, **72**, 115

36 K.-S. Song, S.-K. Kang and S. D. Kim, *Catal. Lett.*,1997, **49**, 65

37 A. M. Venezia, L. F. Liotta, G. Deganello, Z. Schay, D. Horvath and L. Guczi, *Appl. Catal. A,* 2001, **211**, 167

38 E. Gulari, C. Güldür, S. Srivannavit and S. Osuwan, *Appl. Catal. A,* 1999, **182**, 147

39 A. Nagy and G. Mestl, *Appl. Catal. A,* 1999, **188**, 337

40 F. Buatier de Mongeot, A. Cupolillo, M. Rocca and U. Valbusa, *Chem. Phys. Lett.*, 1999, **302**, 302

41 V. I. Bukhtiyarov, V. V. Kaichev and I. P. Prosvirin, *J. Chem. Phys.* 1999, **111**, 2169

42 W. - L. Yim, T. Nowitzki, M. Necke, H. Schnars, P. Nickut, J. Biener, M. M. Biener, V. Zielasek, K. Al - Shamery, Th, Klüner, M. Bäumer, *J. Phys. Chem. C,* 2007, **111**, 445

43 P. J. van den Hoek, E. J. Baerends and R. A. van Santen, *J. Phys. Chem.*, 1989, **93**, 6469

44 J. Biener, A. M. Hodge, J. R. Hayes, C. A. Volkert, L. A. Zepeda-Ruiz, A. V. Hamza and F. F. Abraham, *Nano Lett.* 2006, **6**, 2379

45 A. M. Hodge, J. Biener, J. R. Hayes, P. M. Bythrow, C. A. Volkert and A. V. Hamza, *Acta Mater.*, 2007, **55**, 1343